Inorg. Chem. **2008**, *47*, 11278−11283

A Fluorinated Ruthenium Porphyrin as a Potential Photodynamic Therapy Agent: Synthesis, Characterization, DNA Binding, and Melanoma Cell Studies

Sandya Rani-Beeram,[‡] Kyle Meyer,[†] Anna McCrate,[†] Yiling Hong,[†] Mark Nielsen,[†] and Shawn Swavey*[,‡]

Department of Biology, University of Dayton, 300 College Park, Dayton, Ohio 45469-2320, and Department of Chemistry, University of Dayton, 300 College Park, Dayton, Ohio 45469-2357

Received August 14, 2008

When the new porphyrin 5,10-(4-pyridyl)-15,20-(pentafluorophenyl)porphyrin is reacted with 2 equiv of $Ru(bipy)_2Cl_2$ (where bipy = 2,2′-bipyridine) formation of the target ruthenated porphyrin is achieved with 40% yield. Strong electronic transitions are observed in the visible region of the spectrum associated with the porphyrin Soret and four Q-bands. A shoulder at slightly higher energy than the Soret band is attributed to the Ru(dπ) to bipy(π^*) metal to ligand charge transfer (MLCT) band. The bipyridyl π to π^* transition occurs at 295 nm. Cyclic voltammetry experiments reveal two single-electron redox couples in the cathodic region at $E_{1/2} = -0.80$ and -1.18 V vs Ag/AgCl associated with the porphyrin. Two overlapping redox couples at $E_{1/2} = 0.83$ V vs Ag/AgCl due to the $Ru^{III/II}$ centers is also observed. DNA titrations using calf thymus (CT) DNA and the ruthenium porphyrin give a $K_b = 7.6 \times 10^5\ M^{-1}$ indicating a strong interaction between complex and DNA. When aqueous solutions of supercoiled DNA and ruthenium porphyrin are irradiated with visible light (energy lower than 400 nm), complete nicking of the DNA is observed. Cell studies show that the ruthenated porphyrin is more toxic to melanoma skin cells than to normal fibroblast cells. When irradiated with a 60 W tungsten lamp, the ruthenium porphyrin preferentially leads to apoptosis of the melanoma cells over the normal skin cells.

Introduction

Photodynamic therapy (PDT) is a noninvasive procedure that offers many advantages over traditional cancer treatments.[1] PDT uses light, molecular oxygen, and a photosensitizer to induce cell death.[1] Reactive oxygen species (ROS) are the deleterious agents responsible for cell death.[2] PDT research focused on developing photosensitizers that show little or no dark toxicity, concentrate at tumor sites, and can create ROS indirectly through low-energy illumination are highly coveted. Although many photosensitizers are in clinical trials, only one photosensitizer, Photofrin, is currently approved by the FDA for use in the United States. This drug upon photoexcitation in the visible region of the spectrum generates singlet oxygen from triplet oxygen through energy transfer resulting in cell death.[3] Photofrin however suffers from dark toxicity and purification difficulties,[3] making the search for a replacement very desirable. Many macrocycles particularly porphyrin derivatives have been studied as potential photosensitizers for PDT.[4−9] This is due in part to their affinity for tumor sites,[10] their low dark toxicity, and their intense absorption properties in the visible region of the electromagnetic spectrum.

* To whom correspondence should be addressed. Tel: 1-937-229-3145. Fax: 1-937-229-2635. E-mail: shawn.swavey@notes.udayton.edu.
† Department of Biology.
‡ Department of Chemistry.

(1) Dougherty, T. J.; Gomer, C. J.; Henderson, B. W.; Jori, G.; Kessel, D.; Korbelik, M.; Moan, J.; Peng, Q. *J. Natl. Cancer Inst.* **1998**, *90*, 889.
(2) Macdonald, I. J.; Dougherty, T. J. *J. Porphyrins Phthalocyanines* **2001**, *5*, 105.
(3) Sharman, W. M.; Allen, C. M.; van Lier, J. E. *Drug Discovery Today* **1999**, *4*, 507.
(4) Pandey, R. K. *J. Porphyrins Phthalocyanines* **2000**, *4*, 368.
(5) Hudson, R.; Boyle, R. W. *J. Porphyrins Phthalocyanines* **2004**, *8*, 954.
(6) Wei, W. H.; Wang, Z.; Mizuno, T.; Cortez, C.; Fu, L.; Sirisawad, M.; Naumovski, L.; Magda, D.; Sessler, J. L. *Dalton Trans.* **2006**, 1934.
(7) Chen, X.; Drain, C. M. *Drug Des. Rev.* **2004**, *1*, 215.
(8) Allison, R.; Mota, H.; Sibata, C. *Photodiagn. Photodyn. Ther.* **2003**, *1*, 263.
(9) Allison, R.; Cuenca, R.; Downie, G.; Randall, M.; Bagnato, V.; Sibata, C. *Photodiagn. Photodyn. Ther.* **2003**, *2*, 51.

10.1021/ic8015589 CCC: $40.75
Published on Web 11/04/2008

Another class of compounds that have received a great deal of attention as potential PDT agents are ruthenium complexes containing polypyridyl ligands.[11−13] For example, excitation of the metal to ligand charge transfer (MLCT) state of a Ru(II) polypyridyl complex has been shown to lead to the formation of ROS resulting in efficient cleavage of supercoiled DNA.[14] Ruthenium complexes coordinated to the periphery of porphyrin molecules have also been shown to interact with DNA.[15−22] In one study, a monoruthenated porphyrin caused single-strand breaks of circular plasmid DNA when irradiated with UV light. It was suggested that the mechanism of photocleavage was related to the formation of radical cations of guanine.[17] A separate study of a tetraruthenated porphyrin suggested electrostatic binding to DNA and photocleavage of circular plasmid DNA through formation of singlet oxygen.[20]

Synthetically enhancing porphyrins as PDT agents has been achieved through incorporation of fluorine into the porphyrin structure.[23−26] Halogenated tetraaryl porphyrins combined through a diarylethyne linker (where the halogens were chloro- and fluoro-substituted phenyl groups) had significantly longer excited-state lifetimes compared with their nonhalogenated analogs.[23] As PDT agents, fluorophenyl porphyrins have been efficiently converted to porphyrin−saccharide conjugates to enhance their uptake in cancer cells,[24] while in a separate study, water-soluble fluorinated porphyrins have shown more efficient PDT activity than their nonfluorinated counterparts.[25,26]

We seek to combine the properties of fluorinated porphyrins with those of ruthenium polypyridyl complexes to create a highly active photosensitizer for use in chemotherapy as a photodynamic therapy agent. In this report, we describe the synthesis and characterization by ^{1}H NMR, UV/vis spectroscopy, electrochemistry, and elemental analysis of a new ruthenium porphyrin complex (**I**) and its ability to bind to DNA and photocleave supercoiled DNA when irradiated with low-energy light. In addition, this complex shows low dark toxicity but initiates apoptosis in melanoma cells when irradiated with a 60 W tungsten lamp.

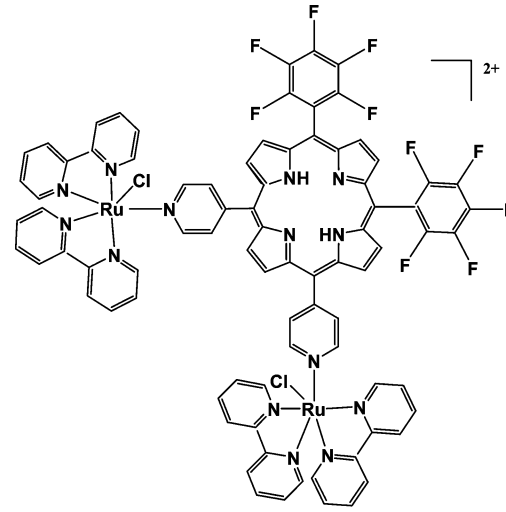

I

Experimental Section

Materials. 4-Pyridylcarboxaldehyde (ACROS), pentafluorobenzaldehyde (ACROS), propionic acid (ACROS), ammonium hydroxide (Fisher), methanol (Fisher), acetone (Fisher), acetonitrile (Fisher), diethylether (Fisher), methylene chloride (Fisher), ethylacetate (Fisher), ethanol (Fisher), $RuCl_3$ trihydrate (Aldrich), 2,2′-bipyridine (Aldrich), 60−200 mesh silica gel (Fisher), ammonium hexafluorophosphate (ACROS), glacial acetic acid (Fisher), tetrabutyl ammonium hexafluorophosphate (Bu_4NPF_6, used as supporting electrolyte for electrochemistry, Aldrich), and ultradry (<50 ppm H_2O) acetonitrile (for electrochemistry measurements, Aldrich) were used without further purification. Pyrrole (Aldrich) was vacuum distilled prior to use. *cis*-$Ru(bipy)_2Cl_2$ was synthesized as previously described.[27] The plasmid pUC18 was obtained from Bayou Biolabs. Electrophoresis-grade low electroendosmosis (EEO) agarose, tris(hydroxymethyl)-aminoethane (Tris), boric acid, and ethidium bromide (EthBr) were obtained from Fisher. The spectroscopic titrations were carried out at room temperature in the buffer 5 mM Tris-HCl, 0.1 M NaCl, pH = 7.2. Concentrations of the calf thymus DNA (Sigma) solutions used in the titrations were determined spectrophotometrically using the extinction coefficient 6600 M^{-1} cm^{-1} at 260 nm.[28] All aqueous solutions were prepared using doubly distilled water. Elemental analyses were performed by Atlantic Microlab, Norcross, Ga. High-resolution mass spectroscopy was performed at the Mass Spectrometry and Proteomics facility, The Ohio State University.

5,10-(4-Pyridyl)-15,20-(pentafluorophenyl)porphyrin [H_2(D-PDPFPP)]. A solution containing 1.9 mL (15 mmol) of pentafluorobenzaldehyde and 4.3 mL (45 mmol) of 4-pyridine carboxaldehyde in 100 mL of propionic acid was heated at reflux for 5 min. Freshly distilled pyrrole (4.2 mL, 60 mmol) was added to this solution, and the reaction mixture was heated at reflux for 2 h.

(10) Tronconi, W.; Colombo, A.; Decesare, M.; Marchesini, R.; Woodburn, K. W.; Reiss, J. A.; Phillips, D. R.; Zumino, F. *Cancer Lett.* **1995**, *88*, 41.
(11) Ang, W. H.; Dyson, P. J. *Eur. J. Inorg. Chem.* **2006**, 4003.
(12) Bergamo, A.; Sava, G. *Dalton Trans.* **2007**, 1267.
(13) Tan, C.; Liu, J.; Chen, L.; Shi, S.; Ji, L. *J. Inorg. Biochem.* **2008**, *102*, 1644.
(14) Mangelli, M. T.; Heinceke, J.; Mayfield, S.; Okyere, B.; Winkel, B. S. J.; Brewer, K. J. *J. Inorg. Biochem.* **2006**, *100*, 183.
(15) Boerner, L. J. K.; Zaleski, J. M. *Curr. Opin. Chem. Biol.* **2005**, *9*, 135.
(16) Gianferrara, T.; Serli, B.; Zangrando, E.; Lengo, E.; Alessio, E. *New J. Chem.* **2005**, *29*, 895.
(17) Mei, W. J.; Liu, J.; Chao, H.; Ji, L. N.; Li, A. X.; Liu, J. Z. *Trans. Met. Chem.* **2003**, *28*, 852.
(18) Zhao, P.; Xu, L. C.; Huang, J. W.; Zheng, K. C.; Fu, B.; Yu, H. C.; Ji, L. N. *Biophys. Chem.* **2008**, *135*, 102.
(19) Onuki, J.; Ribas, A. W.; Medeiros, M. H. G.; Araki, K.; Toma, H. E.; Catalani, L. H.; DiMascio, P. *Photochem. Photobiol.* **1996**, *63*, 272.
(20) Araki, K.; Silva, C. A.; Toma, H. E.; Catalani, L. H.; Medeiros, M. H. G.; Di Masci, P. *J. Inorg. Biochem.* **2000**, *78*, 269.
(21) Narra, M.; Elliott, P.; Swavey, S. *Inorg. Chim. Acta* **2006**, *359*, 2256.
(22) Davia, K.; King, D.; Hong, Y.; Swavey, S. *Inorg. Chem. Commun.* **2008**, *11*, 584.
(23) Yang, S. I.; Seth, J.; Strachan, J.-P.; Gentemann, S.; Kim, D.; Holten, D.; Lindsey, J. S.; Bocian, D. F. *J. Porphyrins Phthalocyanines* **1999**, *3*, 117.
(24) Chen, X.; Hui, L.; Foster, D. A.; Drain, C. M. *Biochemistry* **2004**, *43*, 10918.
(25) Ko, Y. J.; Yun, K. J.; Kang, M. S.; Park, J.; Lee, K. T.; Park, S. B.; Shin, J. H. *Bioorg. Med. Chem. Lett.* **2007**, *17*, 2789.
(26) Zheng, X.; Pandey, R. K. *Anti Cancer Agents Med. Chem.* **2008**, *8*, 241.
(27) Sullivan, B. P.; Salmon, D. J.; Meyer, T. J. *Inorg. Chem.* **1978**, *17*, 3334.
(28) Reichmann, M. F.; Rice, S. H.; Thomas, C. A.; Dotty, P. *J. Am. Chem. Soc.* **1954**, *76*, 3047.

Upon cooling to room temperature, the solution was divided into two fractions, and each fraction was neutralized by cautious addition to a 100 mL 50:50 methanol/ammonium hydroxide solution cooled in an ice bath. The slurry from both fractions was combined, filtered, and air-dried. The fine powder was dissolved in 70−100 mL of ethanol and filtered. The resulting purple powder was air-dried, then dissolved in a minimum of methylene chloride and chromatographed on silica gel using ethyl acetate and ethanol in the ratio 50:50 as the eluent. The first band off the column was 5,15-(4-pyridyl)-10,20-(pentafluorophenyl)porphyrin. The second band off the column was the desired product 5,10-(4-pyridyl)-15,20-(pentafluorophenyl)porphyrin. The second band was collected, and the solvent was removed under reduced pressure giving a purple powder with a yield of 57 mg (0.070 mmol, 0.47% yield). R_f (ethyl acetate/ethanol 50:50) = 0.61. ^{1}H NMR (300 MHz, CD_3CN, TMS): δ 9.09 (4H, dd, 2,6 pyridyl), 8.89 (4H, d, pyrrole), 8.87 (4H, d, pyrrole), 8.20 (4H, dd, 3,5 pyridyl), −2.92 (2H, s, internal pyrrole). UV/vis (CH_3CN) λ_{max} (nm) [$\varepsilon \times 10^{-4}$ M^{-1} cm^{-1}] 410 [18.9], 506 [1.5], 581 [0.62], 648 [0.26]. Anal. Calcd For $C_{42}H_{18}N_6F_{10}\cdot C_2H_5OH$: C, 62.71; H, 2.87; N, 9.97. Found: C, 62.54; H, 3.05; N, 9.86%. TOF-MS ES+ (*m*/*z*; relative abundance): $[C_{42}H_{18}N_6F_{10}]^+$ (796; 100).

***cis*-H_2(DPDPFPP)Ru_2(bipy)$_4Cl_2(PF_6)_2$.** A solution of 0.050 g (0.063 mmol) of *cis*-H_2DPDPFPP and 0.058 g (0.12 mmol) of *cis*-$Ru(bipy)_2Cl_2$ was heated at reflux under nitrogen in 5 mL of glacial acetic acid for 45 min. The glacial acetic acid was removed under reduced pressure, and the residue was taken up in a minimum (5 mL) of methanol and heated at reflux for 45 min. The reaction mixture was added dropwise to 60 mL of an aqueous solution of saturated ammonium hexafluorophosphate, and the precipitate was washed with water. The powder was taken up in a minimum (2 mL) of acetonitrile and flash precipitated by addition to 100 mL of diethylether with stirring. The product was filtered and dried (0.050 g, 0.025 mmol, 40% yield). UV/vis (CH_3CN) λ_{max} (nm) [$\varepsilon \times 10^{-4}$ M^{-1} cm^{-1}] 294 [9.6], 411 [13.9], 507 [2.8], 583 [0.9]. ^{19}F NMR (60 MHz, CH_3CN): δ −67.9 (s, 6F, PF_6), −80.3 (s, 6F, PF_6), −141.0 (m, 4F, ortho), −156.5 (m, 1F, para), −165.0 (m, 4F, meta). Anal. Calcd For $C_{82}H_{50}N_{14}F_{22}\,Cl_2P_2\,Ru_2\cdot 4H_2O$: C, 47.44; H, 2.71; N, 9.19; F, 20.03. Found: C, 47.30; H, 2.51; N, 9.37, F, 19.83%. TOF-MS ES+ (*m*/*z*; relative abundance): $[C_{82}H_{50}N_{14}F_{16}PCl_2Ru_2]^+$ (1839; 46).

Electronic Spectroscopy. Electronic absorption spectra were recorded at room temperature using a Schimadzu 1501 photodiode array spectrophotometer with 2 nm resolution. Samples were run in dry acetonitrile in 1 cm quartz cuvettes.

Electrochemistry. Cyclic voltammograms were recorded using a one-compartment, three-electrode cell, CH-Instruments, equipped with a platinum wire auxiliary electrode. The working electrode was a 2.0 mm diameter glassy carbon disk from CH-Instruments, which was polished first using 0.30 μm followed by 0.05 μm alumina polish (Buehler) and then sonicated for 10 s prior to use. Potentials were referenced to a Ag/AgCl electrode, CH-Instruments. The supporting electrolyte was 0.1 M tetrabutylammonium hexafluorophosphate (Bu_4NPF_6), and the measurements were made in extra dry, <50 ppm water, acetonitrile.

DNA Titrations. Calf thymus (CT) DNA was dissolved in a 5 mM, pH 7.2, tris(hydroxymethyl) aminoethane (Tris) buffer, ionic strength of 0.1 M in NaCl. A stock solution of ruthenium porphyrin (**I**, 19.5 μM) in 10% DMSO was diluted to 9.75 μM using the Tris buffer solution. For DNA titrations, 3.5 mL of the diluted ruthenium porphyrin was placed in 1 cm quartz cuvettes, and aliquots (10 μL) of the CT-DNA solution were added. The Soret band associated with the porphyrin complex was monitored by electronic absorption spectroscopy.

Plasmid Photocleavage. Buffered solutions of pUC18 and pUC18/complex **I** at a ratio of 5:1 bp/metal complex were placed side by side in quartz cuvettes and irradiated with a 100 W mercury arc lamp (Oriel) equipped with a colored glass filter (Newport FSR-GG420) blocking wavelengths shorter than 400 nm. Samples were taken at 15 min intervals over a 2 h period and run in 1% agarose gel by applying 150 V for 1 h in approximately 300 mL of Tris buffer solution. Gels were stained with ethidium bromide and photographed using UV illumination.

Melanoma Cell Studies. The melanoma cell line was obtained from the American Type Culture Collection (ATCC). The cell line is tumorigenic and was obtained from a 53 year old caucasian male. The human skin dermal fibroblast cells were ordered from Promocell (Cat. No. C-12302). Both melanoma and human skin fibroblast cells were cultured in high-glucose DMEM medium, supplemented with 10% fetal bovine serum (FBS), in 5% CO_2 at 37 °C. For porphyrin treatments, melanoma and human skin fibroblast cells were seeded into 6-well plates at a density of 10^5 cells in 3 mL of medium per well. Twenty-four hours later, the growth medium was removed, and the cells in each well were exposed to 1 mL of culture medium containing 5 μM porphyrin solution for 24 h in the dark, followed by light treatment (60 W light bulb) for 30 min. The treated plates were incubated for 1 h. Untreated controls were incubated in parallel. The phase contrast images were acquired by inverted microscope (Nikon TS100) at 10× magnification using MetaMorph Imaging Software.

Results and Discussion

Synthesis and Electronic Absorption. Reactions of the appropriate stoichiometric ratios of 4-pyridine carboxaldehyde and pentafluorobenzaldehyde to give the target porphyrin led to over 90% polymeric byproduct in addition to a statistical distribution of six different porphyrins. Isolation of the porphyrins from the polymeric mix was achieved by washing the precipitate with ca. 100 mL of ethanol. The resulting purple powder was separated into its constituent porphyrins through column chromatography. The yield by this method was low but acceptable under these conditions. Reaction of the *cis*-H_2DPDPFPP porphyrin with 2 equiv of $Ru(bipy)_2Cl_2$[27] gave the desired product, complex **I**, in 40% yield.

Comparison of the electronic transitions of the free base porphyrin (red, Figure 1) and the ruthenated porphyrin **I** (blue, Figure 1) show overlapping intense absorptions at 410 nm indicative of the Soret band. Overlapping less intense Q-bands are present between 500 and 650 nm. The $\pi-\pi^*$ transition associated with the bipyridyl groups occurs for complex **I** at 294 nm with a shoulder at ca. 370 nm attributed to the Ru(dπ) to bipy(π^*) ligand to metal charge transfer (MLCT) transition (blue spectrum, Figure 1). The difference spectrum (inset, Figure 1) is the result of subtracting the spectrum of the free base porphyrin from the spectrum of the ruthenated porphyrin and illustrates more clearly the spectral transitions associated with the coordinated ruthenium groups. The absence of any spectral shifts of the porphyrin transitions upon coordination of the $Ru(bipy)_2Cl^+$ moiety suggests little or no electronic communication between the porphyrin and the peripheral Ru(II) complexes.

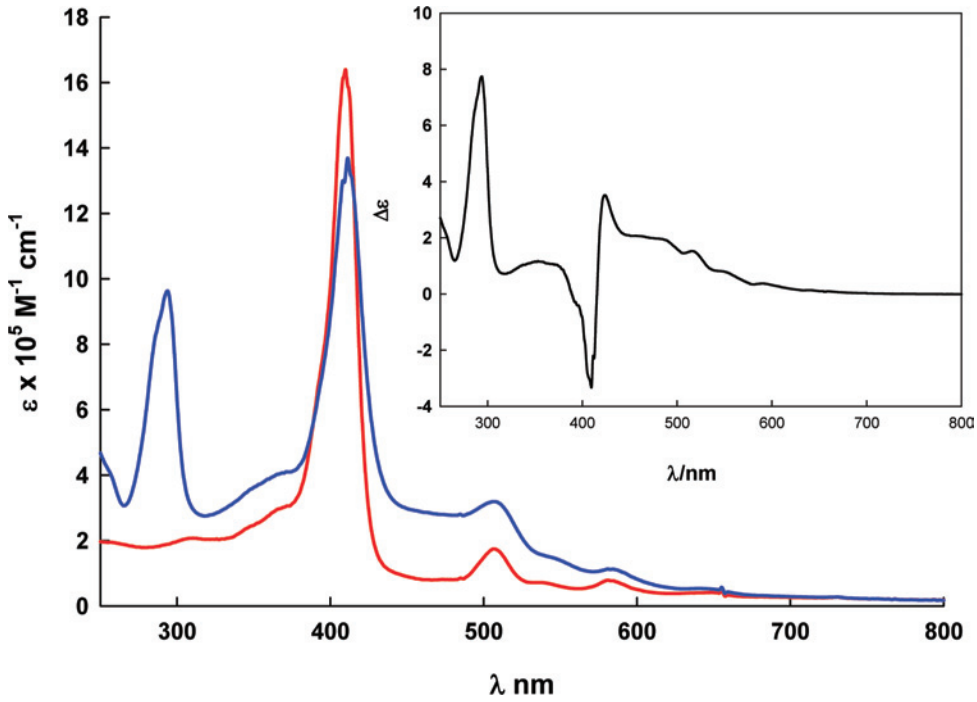

Figure 1. Electronic spectrum of 5,10-(4-pyridyl)-15,20-(pentafluorophenyl)porphyrin (red line) and complex **I** (blue line) in acetonitrile at room temperature. Inset shows the difference spectrum of complex **I** (blue line) and 5,10-(4-pyridyl)-15,20-(pentafluorophenyl)porphyrin (red line).

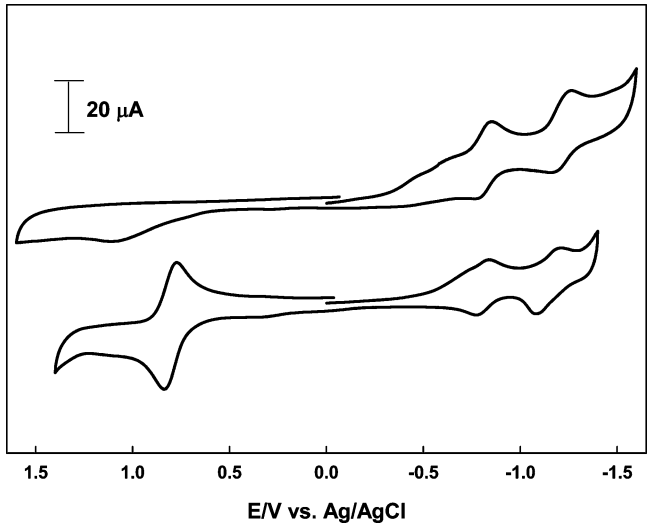

Figure 2. Cyclic voltammograms of 5,10-(4-pyridyl)-15,20-(pentafluorophenyl)porphyrin (top) and complex **I** (bottom) under nitrogen in 0.1 M Bu_4NPF_6 acetonitrile at room temperature. $\nu = 100$ mV/s.

Electrochemistry. Solution-phase cyclic voltammetry (CV) in dry acetonitrile containing Bu_4NPF_6 as supporting electrolyte was performed using a three-electrode cell with a glassy carbon working electrode. Figure 2 illustrates the results of this study. The top cyclic voltammogram is the free base porphyrin, while the bottom one is the ruthenated porphyrin, **I**.

When the free base porphyrin solution is cycled in the cathodic direction, two quasireversible redox couples with $E_{1/2} = -0.86$ V ($\Delta E_p = 110$ mV) and -1.26 V ($\Delta E_p = 110$ mV) vs Ag/AgCl are observed, Figure 2, top. These redox couples are associated with sequential reduction of the porphyrin ring to form radical anions. In the anodic direction, there is a weak irreversible oxidation wave beyond 1.00 V due to oxidation of the porphyrin. Cathodic cycling of the porphyrin ruthenium complex **I** solution reveals two redox couples, a reversible couple with $E_{1/2} = -0.80$ V ($\Delta E_p = 60$ mV) and a quasireversible couple with $E_{1/2} = -1.18$ V ($\Delta E_p = 100$ mV) vs Ag/AgCl attributable to sequential one-electron porphyrin reductions. A reversible redox couple in the anodic region with $E_{1/2} = 0.83$ ($\Delta E_p = 70$ mV) is due to the $Ru^{III/II}$ couple, Figure 2, bottom. The charge ratio of the $Ru^{III/II}$ couple to porphyrin reduction is 2 to 1 in agreement with the structure of complex **I**. The observation of only one $Ru^{III/II}$ redox couple indicates that the Ru(II) metal centers are acting independently of each other. The minor shifts in reduction of the porphyrin upon coordination of the Ru(II) bipyridyl complexes is consistent with the spectral analysis indicating little electronic communication between the porphyrin and the Ru(II) moieties.

DNA Binding Studies. Titrations of pH 7.2 buffer solutions (ionic strength = 0.05 M) of complex **I** with calf thymus (CT) DNA result in a decrease in the Soret band, associated with the porphyrin complex **I**, and a shift to lower energy. Three titration experiments were run, and an example of the resulting spectra for one of these experiments is illustrated in Figure 3. A plot of [DNA]/$\Delta\varepsilon$ versus [DNA] (Scatchard plot) according to eq 1)[29] gives the binding constant K_b. The molar absorptivity ε_a = absorbance/[**I**], ε_b and ε_f are the molar absorptivities of the fully bound and free form of **I**, respectively.

$$[\mathrm{DNA}]/(\varepsilon_a - \varepsilon_f) = [\mathrm{DNA}]/(\varepsilon_b - \varepsilon_f) + 1/[K_b(\varepsilon_b - \varepsilon_f)] \quad (1)$$

The inset of Figure 3 illustrates the results of the Scatchard plot. The binding constant determined by dividing the slope

(29) Assefa, Z.; Vantieghem, A.; Deelereq, Q.; Vandenabeele, P.; Vandenheede, J. R.; Merlevede, W.; deWitte, P.; Agostinis, P. *J. Biol. Chem.* **1999**, *274*, 8788.

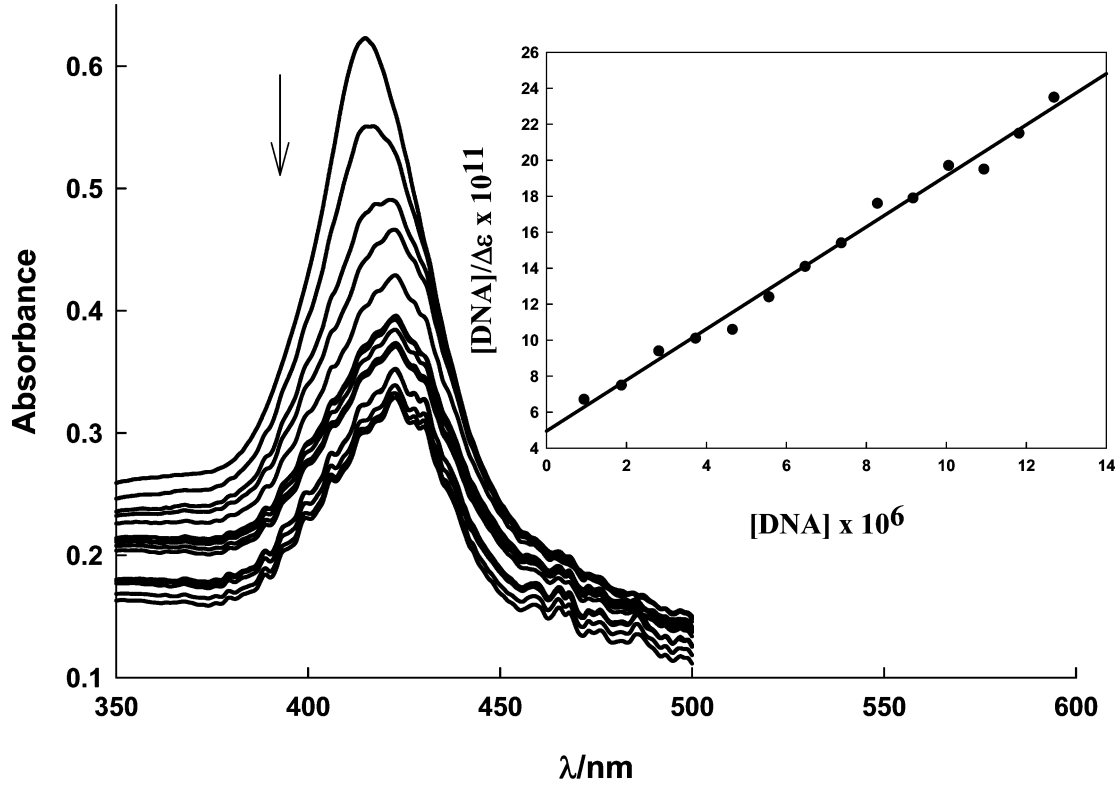

Figure 3. Absorption spectra of pH 7.2 buffer solutions (ionic strength = 0.05 M) of **I** in the presence of increasing amounts of CT-DNA. [**I**] = 10 μM, [DNA] = 0−14 μM. Inset shows a plot of [DNA]/$\Delta\varepsilon$ vs [DNA] from equation **I**.

of the line by the intercept (inset Figure 3) gives a K_b of 7.6 $\times$ 10^5 M^{-1} with an R^2 value of 0.994. The binding constant K_b determined from the three titrations is (6.1 $\pm$ 1.7) $\times$ 10^5 M^{-1}. Binding studies of the free base porphyrin of complex **I** were complicated by low solubility in aqueous solution; however sufficient solubility was obtained with 15% DMSO solutions. Using aqueous 15% DMSO/porphyrin solutions for DNA titrations yielded a binding constant of 2.0 $\times$ 10^4 M^{-1}, considerably less than the binding constant for the ruthenated porphyrin. Previous studies of the polypyridyl ruthenium complex $Ru(bpy)_3^{2+}$ indicate that it binds poorly to DNA mostly through electrostatic interactions.[30]

A shift in the Soret band to lower energy (415 to 423 nm) and the relatively high binding constant is suggestive of an intercalative mode of binding[30,31] for complex **I**; however ethidium bromide displacement experiments indicate that complex **I** does not compete well with ethidium bromide for intercalation into calf thymus DNA suggesting a different mode of binding than intercalation, perhaps groove binding.[32,33] Combination of the free base porphyrin with the Ru(II) moieties does indicate a stronger binding interaction with DNA than the two reactants separately.

DNA Photocleavage Studies. Aqueous solutions of circular plasmid DNA (pUC18, Bayou Biolabs) and **I** at a ratio of 5/1 base pairs (bp)/**I** were irradiated with a 100 W mercury arc lamp equipped with a filter to block out wavelengths less than 400 nm. Samples were removed at 15 min intervals, and gel electrophoresis was performed to determine the ability of **I** to photocleave DNA. Figure 4 illustrates the gel electrophoresis experiment where lanes 1−9 represent the circular plasmid DNA in the absence of complex **I** at various irradiation times. Lane 10 is pUC18/**I**prior to irradiation, and lanes 11−18 represent pUC18/**I** samples taken at 15 min intervals of irradiation. In the absence of complex **I**, the circular plasmid DNA (pUC18, form I) is unaffected by irradiation, lanes 2−9, Figure 4. However after only 15 min of irradiation with visible light (lane 11, Figure 4), the circular plasmid DNA (pUC18) becomes nicked in the presence of complex **I** as indicated by the appearance of form II on the gel. After approximately 1 h of irradiation, the entire supercoiled DNA has been photocleaved. Gel electrophoresis

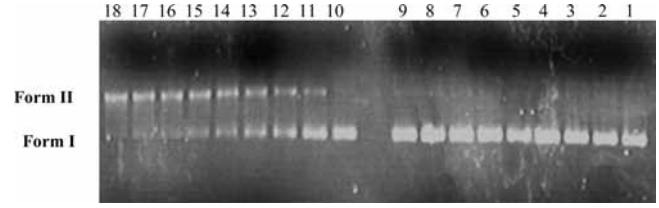

Figure 4. Gel electrophoresis of circular plasmid DNA (pUC18) in the absence (lanes 1−9) and presence (lanes 10−18) of complex **I** at a 5:1 base pair to complex ratio. Lane 1 represents pUC18 prior to irradiation, while lanes 2−9 represent pUC18 irradiated at 15 min intervals. Lane 10 represents pUC18 and complex **I** prior to irradiation, and lanes 11−18 represent pUC18 and complex **I** at 15 min irradiation intervals. Samples were irradiated with a 100 W mercury arc lamp equipped with a long pass filter, cutting off wavelengths below 400 nm. Samples were taken at 15 min intervals.

(30) Pyle, A. M.; Rehman, J. P.; Meshoyrer, R.; Kumar, C. V.; Turro, N. J.; Barton, J. K. *J. Am. Chem. Soc.* **1989**, *111*, 3051.
(31) Sari, M. A.; Battioni, J. P.; Dupre, D.; Mansuy, D.; LePeeq, J. B. *Biochemistry* **1990**, *29*, 4205.
(32) McMillin, D. R.; Shelton, A. H.; Bejune, S. A.; Fanwick, P. E.; Wall, R. K. *Coord. Chem. Rev.* **2005**, *249*, 1451.
(33) Biver, T.; Secco, F.; Venturini, M. *Coord. Chem. Rev.* **2008**, *252*, 1163.

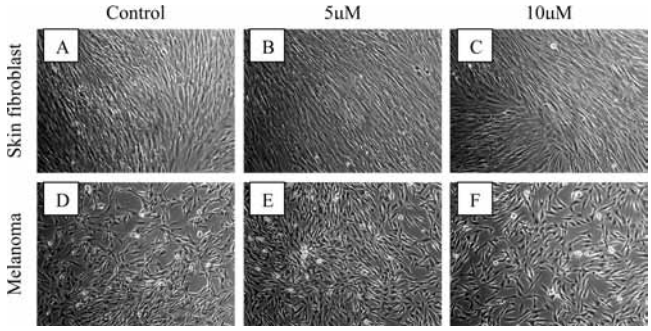

Figure 5. Phase-contrast microscope images of cells incubated in the dark for 1 day. Skin fibroblast cells without complex **I** (A) and with complex **I** at 5 and 10 μM concentrations (B, C) and melanoma cells without complex **I** (D) and with complex **I** at 5 and 10 μM concentrations (E, F).

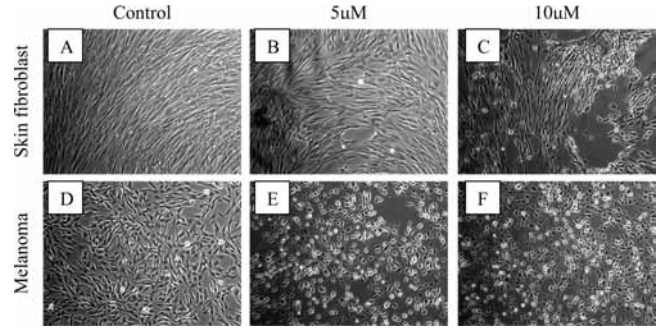

Figure 6. Phase-contrast microscope images of cells irradiated with a 60 W tungsten lamp for 30 min and then incubated for a 1 h period. Skin fibroblast cells without complex **I** (A) and with complex **I** at 5 and 10 μM concentrations (B, C) and melanoma cells under the same conditions without complex **I** (D) and with complex **I** at 5 and 10 μM concentrations (E, F).

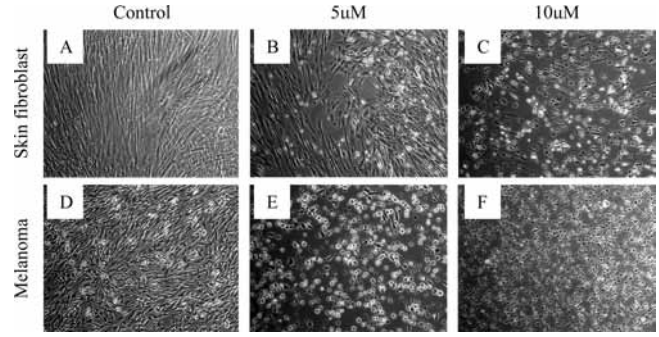

Figure 7. Phase-contrast microscope images of cells irradiated with a 60 W tungsten lamp for 30 min and then incubated for a 12 h period. Skin fibroblast cells without complex **I** (A) and with complex **I** at 5 and 10 μM concentrations (B,C) and melanoma cells under the same conditions without complex **I** (D) and with complex **I** at 5 and 10 μM concentrations (E,F).

experiments in the absence of light irradiation revealed no difference between the circular plasmid DNA with and that without complex **I**, confirming that the process observed is light-induced. When irradiated for 1 h with a 50 W halogen lamp, pUC18 in the presence of the free base porphyrin does not show appreciable DNA photocleavage.

Cell Studies. Skin fibroblast and melanoma cells were placed in well plates, and once the cells were confluent, designated wells were treated with complex **I** at 5 μM and 10 μM. As a control, the normal and melanoma cells were cultured in the absence of complex **I**, Figure 5A,D, respectively. To determine the dark toxicity of the complex, the cells were incubated with complex **I** for one day in the dark. At concentrations of 5 and 10 μM of complex **I** (incubated in the dark), normal skin cells and melanoma cells do not present significant apoptosis, Figure 5, panels B and E and C and F, respectively. Cell studies of a tetraruthenated pyridyl porphyrin[34] on the other hand show complete apoptosis of both normal and melanoma cells when incubated in the dark under the conditions described herein, suggesting a clear link between the number of pendant ruthenium complexes and cell toxicity.

The light experiments were performed on skin and melanoma cells in the presence and absence of complex **I**. The cells were placed in well plates, and once the cells were confluent, designated wells were treated with complex **I** at 5 and 10 μM as before. After 24 h of incubation following treatment, the cells were irradiated with a 60 W tungsten lamp for 30 min and then incubated for a 1 h period (Figure 6) and a 12 h period (Figure 7). Significant apoptosis is not observed upon irradiation of the skin fibroblast and melanoma cells in the absence of complex **I** for the 1 h (Figure 6A,D) and 12 h (Figure 7A,D) incubation periods. Skin fibroblast cells in the presence of complex **I** at 5 μM irradiated for 30 min and incubated for 1 h (Figure 6B) show little effect compared with the skin fibroblast cells in the absence of complex **I** (Figure 6A). Melanoma cells, on the other hand, show nearly complete apoptosis when irradiated in the presence of complex **I** at 5 μM and incubated for 1 h (Figure 6E). The skin fibroblast cells at 10 μM complex **I** concentration (Figure 6C) present more cell death than skin cells at the 5 μM concentration (Figure 6B) but significantly less apoptosis than melanoma cells exposed to complex **I** at both 5 (Figure 6E) and 10 μM (Figure 6F). This indicates that the apoptotic effect is concentration dependent and preferential to melanoma cells.

Conclusions

A new porphyrin and ruthenated porphyrin have been presented. Electronic absorption and electrochemical studies indicate that there is little electronic communication between the orbitals of the peripheral ruthenium metal centers and the orbitals associated with the porphyrin. DNA binding studies indicate a strong interaction between the metal−porphyirn complex and double-stranded DNA. When solutions of the complex and supercoiled DNA were irradiated with visible light >400 nm, complete nicking of the supercoiled DNA was observed. Cell studies indicate low dark toxicity for complex **I** toward both melanoma and normal cells. Normal cells are only slightly affected by the combination of complex **I** and visible light, in contrast to melanoma cells in the presence of complex **I** and visible light, which reveal extensive apoptosis. This suggests a preference of complex **I** for melanoma cells. Further studies are underway to elucidate the mechanism of cell death.

Acknowledgment. The authors would like to thank Dr. Mark Masthay and Aaron Beach for help with the irradiation experiments and Dr. Howard Knachel for his help with the fluorine NMR. We would also like to thank the generous contributions of the "Merck Institute for Science Education" for support of this work.

IC8015589

(34) Araki, T.; Toma, H. E. *J. Coord. Chem.* **1993**, *30*, 9.